

# Y-Shaped Microfluidic Fuel Cell with Novel Cathode Structure

M. S. Feali\*

Department of Electrical Engineering, Kermanshah Branch, Islamic Azad University, Kermanshah, Iran

\*e-mail: msaeed.feali@gmail.com

Received July 13, 2021; revised October 15, 2021; accepted November 11, 2021

**Abstract**—Due to low oxygen solubility in the electrolyte, creating a depletion layer on the cathode surface is an important factor in reducing the performance of the microfluidic fuel cell. In this paper, for improving the mass transfer to the surface of the cathode in the Y-shaped microfluidic fuel cell with a flow over structure, a novel cathode structure is presented. Here, the conventional cathode is divided into smaller parts, and these parts are placed in the path of the oxidant flow. We consider the microfluidic fuel cell with liquid phase fuel and oxidant streams operate at room temperature  $T = 298$  K. Results show that due to the appropriate mass transfer rate to the surface of the proposed cathode, the possibility of the formation of the depletion area on the cathode surface is reduced. In the proposed structure of the cathode, both the initial parts of the cathode and the end parts of the cathode play a role in generating electric current, and as a result, the output current density of the cell increases. The results show that the electric current density and the peak power density of the proposed cell are significantly higher than conventional cells at both low and high reactant flow rates.

**Keywords:** microfluidic, fuel cell, cathode

**DOI:** 10.1134/S1023193522070060

## INTRODUCTION

The desire to build smaller electronics has made the need to build innovative power-generating devices even more important. Micropower generation is a small-scale energy conversion scheme to power portable devices [1]. These applications include not only common facilities such as laptop computers and cell phones, but also more specialized devices such as diagnostic and clinical tests, microanalytical devices for field tests, and global positioning systems.

Micro fuel cells are good options for generating electricity for modern electronics and can be widely used in portable electronics [2, 3]. Fuel cells have advantages over conventional Li-batteries, such as continuous power generation as long as the fuel and oxidizer are supplied, longer lifetime, higher reliability, and the ability to integrate with the system.

One of the types of fuel cells that have recently been considered is microfluidic fuel cells. In the microfluidic fuel cells, there is no need for a membrane to separate the oxidant flow from the fuel flow. In the microfluidic channel due to the microscale size of the channel, the flow is laminar. Here, a stable liquid interface exists in co-laminar flow while the only fluid transfer process perpendicular to the direction of the flow is diffusion [4]. So, in microfluidics, two fluids can flow together without mixing. Therefore, some of the membrane-related problems in fuel cells such as membrane degradation, losses in ion transfer, humidification, dry out, and membrane degradation are

minimized [5]. Most importantly, the overall dimensions of the cell are reduced, and the cell structure will be a simple single-layer structure like common lab-on-chip devices. The single-layer structure can be fabricated using conventional microfabrication or micro-machining techniques. In addition, miniaturization of the fuel cell will increase the surface-to-volume ratio, thereby increasing the output power density of the fuel cell because the reactions in the fuel cells are surface-based. Additionally, removing the membrane in the microfluidic fuel cells considerably decreases the cost of fabrication. These cells may be used in lab-on-chip and portable electronic devices.

Microfluidic fuel cells have some drawbacks such as the creation of a depletion boundary layer on the electrode surface, mixing at the fuel oxidant interface, and low oxygen solubility in the electrolyte [5, 6]. At the fuel oxidant interface, due to the diffusion transfer process, the two fluids are mixed so that the width of the mixing area increases with increasing cell length. The mixing area causes two defects: (1) the concentration of fuel at the anode surface decreases, (2) the open-circuit voltage decreases due to mixed potential at cathode and fuel crossover. The mixing of fuel and electrolyte at the interface can lead to the fuel occurring at the cathode surface. Therefore, both the reduction reaction and oxidation reaction occur on the cathode, leading to mixed potential on the cathode, thus the output voltage drops down. Another factor in reducing the performance of the microfluidic fuel cell

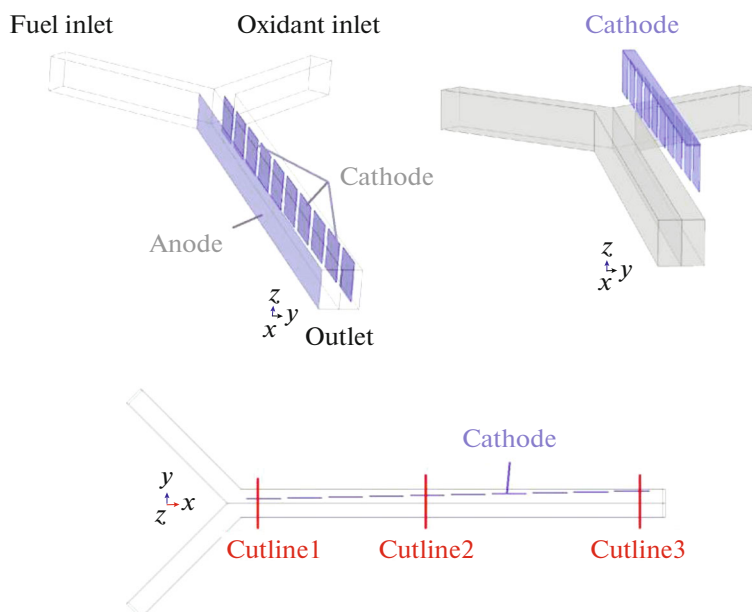


Fig. 1. Schematic of the proposed Y-shaped microfluidic fuel cell with a new cathode structure.

is the creation of the depletion boundary layer at the surface of the electrodes [6]. Due to the lack of a convection transfer process perpendicular to the flow, the only transfer process that can bring the reactive particles to the surface of the electrodes is the diffusion transfer process. However, the diffusion transfer process is very limited and can not bring the new reactant particles to the surface of the electrodes at an appropriate rate, thus during the cell operation, a depletion boundary layer is created on the electrode surface, which reduces the electric current density of the cell. Creating a depletion layer on the cathode surface due to the low solubility of oxygen in the electrolyte is another factor in reducing the performance of the microfluidic fuel cell. To address this issue, solutions with high solubility and high concentration of oxygen, such as hydrogen peroxide [7] and vanadium redox couples [8] were utilized.

Various microfluidic fuel cells with side-by-side streaming architectures have been reported to decrease the depletion area on the surface of the electrodes by increasing the rate of mass transfer to the surface of the electrodes. The results of several researches show that the mass transfer to the electrode surface correlates with the geometric configuration. Manipulation of inputs and outputs locations [9, 10], dividing the microchannel length into multiple segments [11], multi-stream structure [12, 13], and manipulation of the flow structure and transport pattern [10, 14] are different ways to improve the mass transfer to the surface of the electrodes and reduce the depletion layer. Manipulating the architecture of the electrodes is another way to reduce the depletion boundary layer [5, 15–17]. By changing the location

and shape of the electrodes, the transfer of mass to their surface can be increased, thus preventing the formation of a depletion layer on the surface of the electrodes.

In this paper, a new cathode structure is proposed to reduce the depletion area on the cathode surface. Using a numerical macro-scale model, the performance of the proposed microfluidic fuel cell is evaluated.

## NUMERICAL MODELING

### *Computational Domain*

Figure 1 schematically shows the computational domain. Fuel and oxidant fluids are introduced into a microchannel through two separate inlets which form a side-by-side co-laminar flow. This fuel cell uses flow-over electrode architecture. The anode is simply located on the channel wall. Because of the low oxygen solubility in the electrolyte, the possibility of creating a depletion layer on the surface of the cathode is much higher than that of the anode, and this limits the electrical current produced by the cell. Therefore, to reduce the possibility of creating a depletion layer on the cathode surface, we change the structure of the cathode in such a way that oxygen particles in the electrolyte body reach the cathode surface at a suitable rate. For this purpose, we divide the cathode into smaller parts and place these parts in the path of the electrolyte flow so that the parts at the beginning of the channel are near the fuel oxidant interface and the parts at the end of the channel are close to the channel wall (Fig. 1). In this structure, the cathode is less in contact with the mixing area, because as the width of the mixing area increases, the cathode parts also move

**Table 1.** Geometric parameters of the cell

Parameters	Value, mm
Main flow channel length × height × width	15 × 1 × 1
Each of the Inlet channels length × height × width	5 × 1 × 0.7
Outlet height × width	1 × 1
Each part of cathode length × height × width	1.2 × 1 × 0.02
Displacement of each cathode relative to the adjacent cathode in the <i>x</i> direction	1.45
Displacement of each cathode relative to the adjacent cathode in the <i>y</i> direction	0.03

away from the fuel-oxidant interface. There are other ways to improve cell efficiency, such as using an air-breathing cathode or other oxidants with high solubility, but our goal is to show how effective the cathode geometric design will be in improving cell performance. Regarding the fabrication issues of this particular cathode structure, the proposed cathode can be easily fabricated by methods such as 3D printing.

Details of the geometric parameters of the cell are listed in Table 1. The proposed macro-scale model is developed with COMSOL Multiphysics. Governing equations in fuel cell simulation are formulated based on the conservation laws for mass, momentum, species, and electrical potentials. Using the Butler–Volmer equation these equations are coupled together.

**Table 2.** Parameters used in the model [5]

Parameter	Anodic flow	Cathodic flow
Flow rate	500 μL min <sup>-1</sup>	500 μL min <sup>-1</sup>
Density	1000 kg m <sup>-3</sup>	1840 kg m <sup>-3</sup>
Dynamic viscosity	0.0017 Pa s	0.0267 Pa s
Faraday constant	96485.34 C mol <sup>-1</sup>	96485.34 C mol <sup>-1</sup>
Cell temperature	298 K	298 K
Universal gas constant	8.314 J mol <sup>-1</sup> K <sup>-1</sup>	8.314 J mol <sup>-1</sup> K <sup>-1</sup>
Conductivity	11.47 S m <sup>-1</sup>	43 S m <sup>-1</sup>
Charge transfer coefficient	0.5	0.5
Number of electrons transferred	2	4
Exchange current density	3.82 × 10 <sup>+5</sup> A m <sup>-3</sup>	100 A m <sup>-3</sup>
Inlet concentration	2100 mol m <sup>-3</sup>	0.5 mol m <sup>-3</sup>
Diffusion coefficient	8.3 × 10 <sup>-10</sup> m <sup>2</sup> s <sup>-1</sup>	8.3 × 10 <sup>-10</sup> m <sup>2</sup> s <sup>-1</sup>

*Fluid Flow*

Due to its small dimensions, in the microchannel, the flow is assumed to be laminar and incompressible. The flow filed in the microchannel is governed by Navier–Stokes and continuity equations [18]:

$$\begin{aligned} \nabla \vec{u} &= 0, \\ \rho(\vec{u}\nabla\vec{u}) &= -\nabla p + \mu\nabla^2\vec{u}. \end{aligned} \quad (1)$$

Where *u* is the velocity, *p* the pressure,  $\rho$  the fluid density and  $\mu$  is the dynamic viscosity. The density and viscosity of the fluid are assumed to be constant. Detailed model parameters are listed in Table 2. Normal inflow boundary condition with identical velocities is determined at the two inlets, while atmospheric pressure is considered for the outlets. On the walls of the channel, the no slip boundary condition is considered.

*Mass Transport*

Concentration distributions of the fuel and oxidant in the microchannel is governed by convective–diffusion equation [18] given as:

$$\nabla(-D\nabla c + c\vec{u}) = 0. \quad (2)$$

Where *c* is the local concentration of the reactants. Velocity field within the microchannel is determined by Navier–Stokes equations.

Here, the catalyst layers are assumed to be as the boundaries where the corresponding electrochemical reactions take place over these boundaries. Thus, the boundary condition for these boundaries is:

$$n(-D\nabla c + c\vec{u}) = \frac{i}{nF}, \quad (3)$$

where  $i$  reflects the current density which is calculated by Butler–Volmer equation,  $F$  is the Faraday constant,  $n$  denotes the number of electrons transferred in the reaction and  $\mathbf{n}$  is the normal vector.

The right side of the above equation indicates the consumption rate of species over the electrodes.

At the inlets, the constant concentration boundary condition is considered. At the outlets, the convective flow boundary condition is considered. No flux boundary condition is set to all other boundaries.

### Charge Conservation

To calculate the electrical potential within the electrolyte and electrodes, following equations can be used:

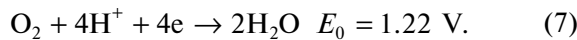
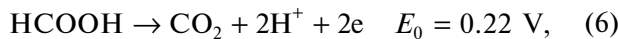
$$\sigma_{\text{elyt}} \nabla \cdot \nabla \phi_{\text{elyt}} = 0, \quad (4)$$

$$\sigma_{\text{eltd}} \nabla \cdot \nabla \phi_{\text{eltd}} = 0, \quad (5)$$

where  $\sigma_{\text{elyt}}$  is the electrolyte conductivity,  $\sigma_{\text{eltd}}$  is the electrodes conductivity,  $\phi_{\text{elyt}}$  and  $\phi_{\text{eltd}}$  are the local potential in the electrolyte and electrodes respectively. Because the thickness of catalyst layer is about 10  $\mu\text{m}$  so it is negligible and in modeling it can be assumed as a boundary layer. The anode boundary layer is set to zero potential, and the cathode boundary layer is set to the cell voltage. All other boundaries are set to insulation boundary condition.

### Electrochemical Kinetics

The electrical current generates in fuel cells by electrochemical reactions at the anode and cathode surfaces. In the proposed microfluidic fuel cell the oxidation of formic acid and reduction of oxygen is presented as:



The generated local current density,  $i$ , across the electrode surface is calculated by Butler–Volmer equation [19]:

$$i = i_0 \frac{c}{c_{\text{REF}}} \left[ e^{(\alpha n F / RT) \eta} - e^{-(1-\alpha) n F / RT \eta} \right] - 2FN_{\text{crossover}}, \quad (8)$$

where  $c_{\text{REF}}$  is the reference reactant concentration,  $i_0$  the exchange current density at the reference reactant concentration,  $\eta$  the overpotential,  $\alpha$  the charge transfer coefficient,  $R$  the universal gas constant,  $T$  the operating temperature considered as a constant parameter, and  $N_{\text{crossover}}$  is the fuel crossover flux at the cathode surface.

At each electrode, overpotential is:

$$\eta = \phi_{\text{eltd}} - \phi_{\text{elyt}} - E_{\text{REVERSIBLE}}, \quad (9)$$

where  $E_{\text{REVERSIBLE}}$  is the reversible potential.

### Solution Procedure

Graphical user interface and pre-programmed modules of COMSOL Multiphysics are used for developing the proposed macro-scale model of the microfluidic fuel cell. The equations of fluid flow, mass conservation, charge conservation, and electrochemical reaction kinetics are solved using COMSOL Multiphysics. The COMSOL modules of transport of Diluted Species (tds), laminar flow (spf), and electric currents (ec) are used to model the microfluidic fuel cell. At first, the fluid flow equations are solved. Then, the fluid flow data is used to solve the coupled mass and charge transport with electrochemical reactions. To discretize the device geometry, the triangular mesh pattern with fine element size is used to ensure that the accuracy of the calculations is high enough and it does not depend on the mesh size. To achieve accurate results, refined meshes were used in the electrodes. The stationary segregated Multifrontal Massively Parallel Solver (MUMPS) is used to solve the equations of transport of Diluted Species (tds), laminar flow (spf), and electric currents (ec) modules. The electrical current output of the cell is calculated using integrating the reaction current density on the surface of the anode. The simulations are performed using Core i5-2500k 3.30 GHz processor with 8 GB of RAM.

## RESULTS AND DISCUSSIONS

### Model Validation

To validate the numerical model, the fuel cell in experimental work [5] is simulated using the model and then the experimental results are compared with the simulation results. Figure 2 shows the polarization curves obtained from the simulation and experiment. To evaluate the simulation accuracy, we calculate the root mean square error and correlation between the experimental and the simulated results of output current densities. The root mean square error is:

$$\text{RMSE} = \sqrt{\frac{\sum_{i=1}^n (i_{\text{exp}} - i_{\text{sim}})^2}{n}}, \quad (10)$$

where  $i_{\text{exp}}$  and  $i_{\text{sim}}$  are the experimental and simulated current densities, respectively.  $n$  is the number of data points in the polarization curve.

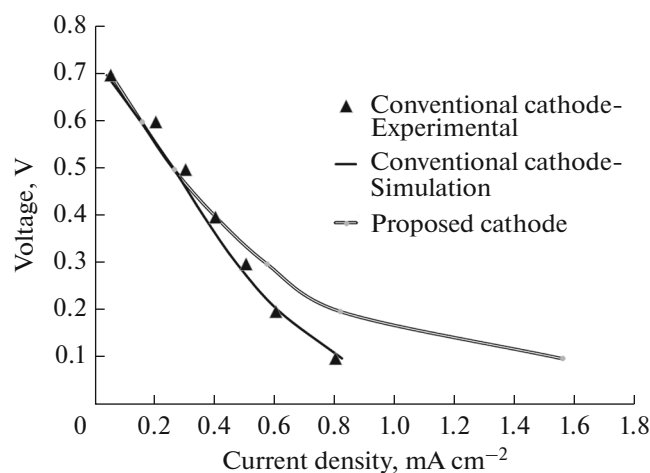


**Fig. 2.** The polarization curves of the cell with conventional flow over cathode obtained from the simulation and experiment [5], and the polarization curve of proposed cell with the new cathode structure.

The correlation is defined as:

$$\text{Corr} = \frac{\sum_{i=1}^n (i_{\text{exp}} - \overline{i_{\text{exp}}})(i_{\text{sim}} - \overline{i_{\text{sim}}})}{\sqrt{\sum_{i=1}^n (i_{\text{exp}} - \overline{i_{\text{exp}}})^2} \sqrt{\sum_{i=1}^n (i_{\text{sim}} - \overline{i_{\text{sim}}})^2}}. \quad (11)$$

The root mean square error of 0.032 and the correlation coefficient of 0.996 confirms the accuracy of the numerical model.

### Cell Performance

Compared to the conventional flow over cathode structure in [5], in the proposed cathode structure the geometric shape has changed in such a way that the cathode is divided into smaller parts. In addition, the location of the cathode parts is adjusted so that the oxygen particles can reach the surface of the cathode parts at a reasonable rate. The overall size of the proposed cathode is approximately the same as a conventional cathode. Figure 2 shows the polarization curves of the cell in [5] with conventional flow over cathode and the proposed cell with the new cathode structure. Comparison of these two curves shows that the proposed cathode structure has a great effect on increasing the output current density of the fuel cell.

Polarization and power density curves of the proposed fuel cell for three different flow rates are shown in Fig. 3. The results show that the proposed cathode can also perform well at low fluid flow rates. The results show that the effect of the geometry of the proposed cathode on improving the performance of the cell is more evident at low flow rates as well as at low voltages. In fact, at low voltages (due to the high rate of

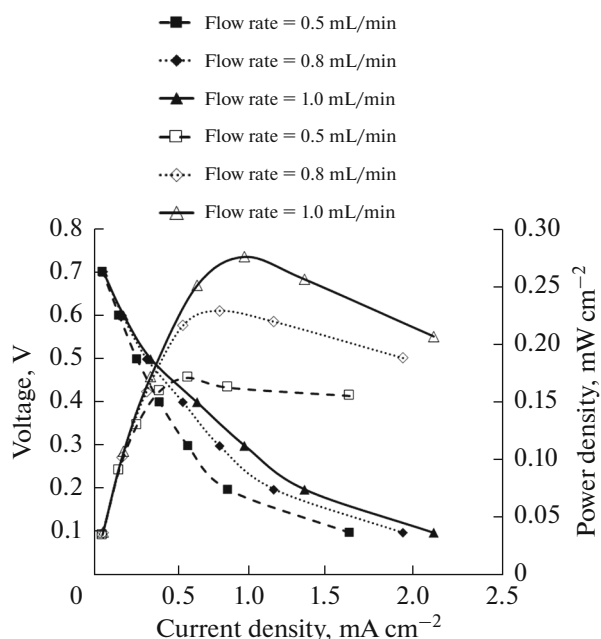


**Fig. 3.** Polarization and power density curves of the proposed fuel cell for three different flow rates.

reactant consumption and also at low reactant flow rates due to low mass transfer rate, the possibility of forming a depletion area at the surface of the cathode is high. Therefore, in both cases, there is a greater need for the high mass transfer rate to the cathode surface. As a result, the effect of the geometric structure of the cathode in improving the output current density of the cell is more obvious in these two cases, at low flow rates as well as at low voltages.

### Concentration Distribution of Reactants

To investigate the possibility of the fuel crossover problem, Fig. 4 shows the fuel concentration change curve across the different cut lines for the flow rate of 0.5 mL/min. These curves show that the upstream parts of the cathode are in minimal contact with the fuel. Also, the fuel concentration near the cathode is not critical for downstream cathodes. Figure 5 shows the concentration distribution of oxygen at the channel cross-sections for the flow rate of 0.5 mL/min at the cell voltage of 0.4 V. This figure shows that the formation of the depletion layer on the surface of the cathode is not significant. Due to the special arrangement of the cathode, the reactants can reach the cathode surface at a suitable rate, thus the possibility of the formation of a depletion area on the cathode surface is reduced. Figure 6 shows the oxygen concentration change curve across the different cut lines at different cell voltages for the flow rate of 0.5 mL/min. As can be seen from each of these graphs, the concentration of oxygen on the cathode surface at different distances

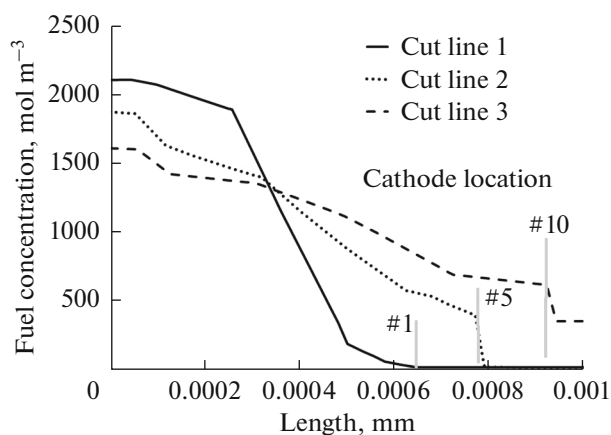


Fig. 4. Fuel concentration change curve across the different cut lines for flow rate of 0.5 mL/min, at cell voltage of 0.1 V.

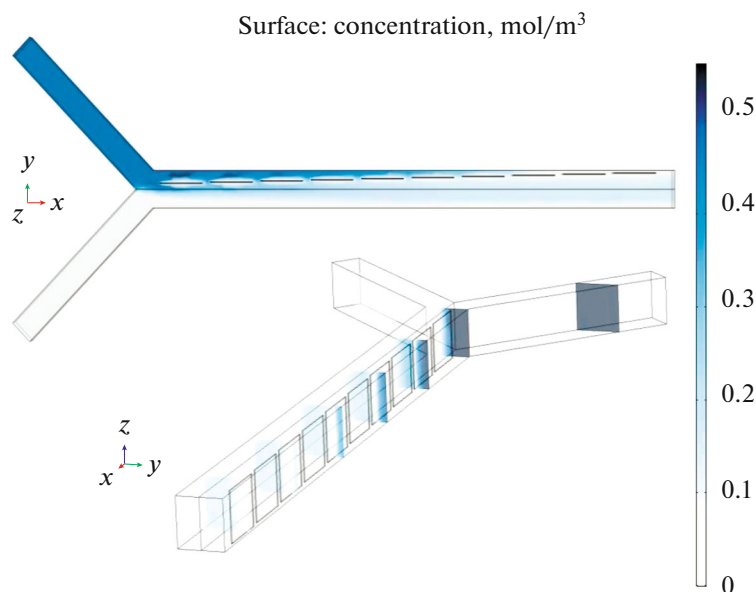


Fig. 5. The concentration distribution of oxygen at the channel cross sections for flow rate of 0.5 mL/min at cell voltage of 0.4 V.

from the channel input is not significantly different. This indicates that the cathode structure allows oxygen particles to reach all parts of the cathode (near or far from the inlet) at a reasonable rate. In the proposed structure of the cathode, both the initial parts of the cathode and the end parts of the cathode play a role in generating electric current, and as a result, the output current density of the cell increases. While in typical fuel cell structures with a long cathode in the sidewall, creating a depletion layer on the cathode surface prevents fresh oxygen particles to reach the end parts of the cathode, and as a result, this part of the cathode has almost no role in generating electricity.

The electric current production of each cathode at the cell voltage of 0.4 V is shown in Fig. 7. The results

show that all cathodes contribute to the production of electric current.

#### *Effect of Reactant Flow Rates on the Cell Performance*

Figure 8 shows the effect of the flow rates on the current density and the peak power density of the cell. This figure shows that the electric current density of the cell is increased by increasing the flow rate at the inlets of the cell. As can be seen, the limitation of mass transfer is evident at low flow rates due to insufficient oxidant supply. In fact, increasing the fluid flow rate at the inlet improves mass transfer to the electrode surface. As shown in Fig. 8, increasing the flow rate of the fluid also increases the peak power density of the cell.

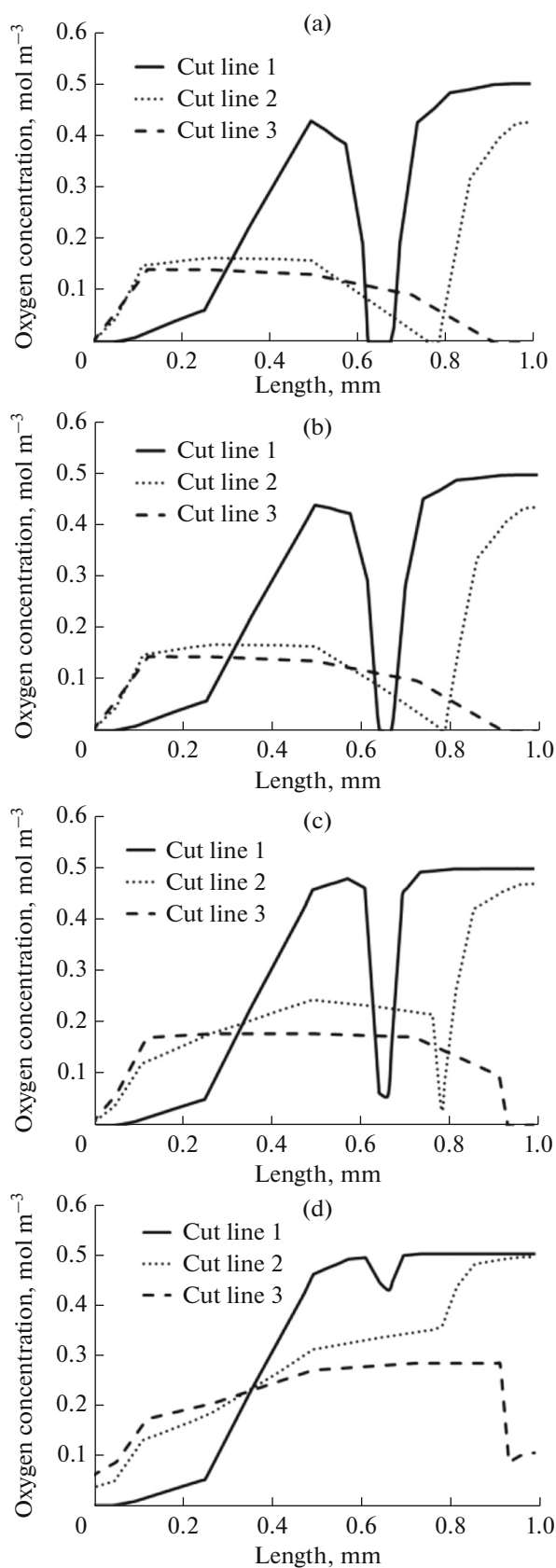


**Fig. 6.** Oxygen concentration change curve across the different cut lines for flow rate of 0.5 mL/min, at cell voltage of (a) 0.1 V, (b) 0.3 V, (c) 0.5 V, and (d) 0.7 V.

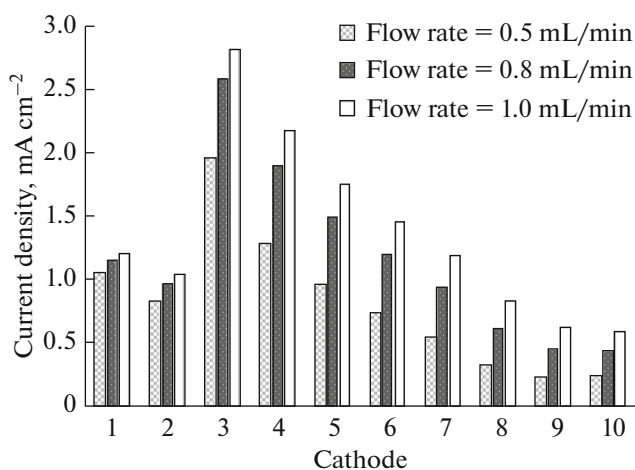


**Fig. 7.** The electric current production of each cathode at cell voltage of 0.4 V.

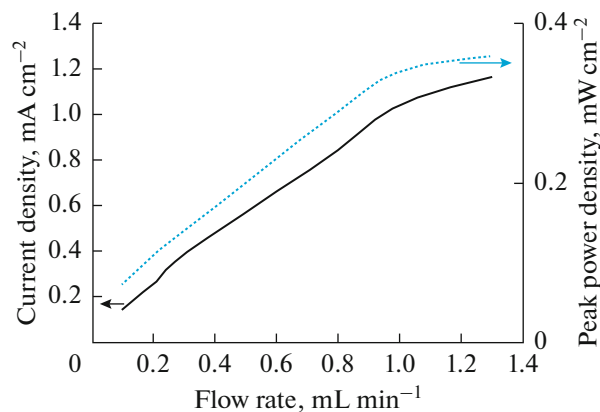


**Fig. 8.** The effect of the flow rates on the current density (at 0.3 V cell voltage) and the peak power density of the cell.

## CONCLUSIONS

In this paper, a novel cathode structure is presented for improving the mass transfer to the surface of the cathode in the Y-shaped microfluidic fuel cell. The proposed cathode structure consists of several small cathodes placed in the flow path of the oxidant in such a way that they have maximum contact with the body of the oxidant fluid. The simulation of the concentration distribution of reactants shows that due to the specific structure of the proposed cathode, the mass transfer rate to the surface of small cathodes is high and as a result, the possibility of creating a depletion area on the surface of these cathodes is minimized. In the proposed structure, because the depletion area does not form on the surface of the small cathodes, all of the small cathodes play a role in generating an electric current. The results show that the electric current density and the peak power density of the proposed

cell are significantly higher than conventional cells at both low and high reactant flow rates.

#### CONFLICT OF INTEREST

The authors declare that they have no conflict of interest.

#### REFERENCES

1. Chou, S.K., Yang, W.M., Chua, K.J., Li, J., and Zhang, K.L., Development of micro power generators—a review, *Appl. Energy*, 2011, vol. 88, p. 1.
2. Yousfi-Steiner, N., Moçotéguy, P., Candusso, D., and Hissel, D., A review on polymer electrolyte membrane fuel cell catalyst degradation and starvation issues: causes, consequences and diagnostic for mitigation, *J. Power Sources*, 2009, vol. 194, no. 1, p. 130.
3. Wang, Y., Leung, D.Y., Xuan, J., and Wang, H., A review on unitized regenerative fuel cell technologies, part-A: unitized regenerative proton exchange membrane fuel cells, *Renew. Sust. Energy Rev.*, 2016, vol. 65, p. 961.
4. Morse, J.D., Micro-fuel cell power sources, *Int. J. Energy Res.*, 2007, vol. 31, p. 576.
5. Choban, E.R., Markoski, L.J., Wieckowski, A., and Kenis, P.J., Microfluidic fuel cell based on laminar flow, *J. Power Sources*, 2004, vol. 128, p. 54.
6. Choban, E.R., Waszczuk, P., and Kenis, P.J., Characterization of limiting factors in laminar flow-based membraneless microfuel cells, *Electrochem. Solid State Lett.*, 2005, vol. 8, p. A348.
7. Kjeang, E., Brolo, A.G., Harrington, D.A., Djilali, N., and Sinton, D., Hydrogen peroxide as an oxidant for microfluidic fuel cells, *J. Electrochem. Soc.*, 2004, vol. 154, p. B1220.
8. Kjeang, E., McKechnie, J., Sinton, D., and Djilali, N., Planar and three-dimensional microfluidic fuel cell architectures based on graphite rod electrodes, *J. Power Sources*, 2007, vol. 168, p. 379.
9. Salloum, K.S., Hayes, J.R., Friesen, C., and Posner, J.D., Sequential flow membraneless microfluidic fuel cell with porous electrodes, *ECSTrans.*, 2008, vol. 13, p. 21.
10. Yoon, S.K., Fichtl, G.W., and Kenis, P.J., Active control of the depletion boundary layers in microfluidic electrochemical reactors, *Lab. Chip*, 2006, vol. 6, p. 1516.
11. Rizvandi, O.B. and Yesilyurt, S., Modeling and performance analysis of branched microfluidic fuel cells with high utilization, *Electrochim. Acta*, 2019, vol. 318, p. 169.
12. Sun, M.H., Casquillas, G.V., Guo, S.S., Shi, J., Ji, H., Ouyang, Q., and Chen, Y., Characterization of microfluidic fuel cell based on multiple laminar flow, *Microelectron. Eng.*, 2007, vol. 84, p. 1182.
13. Lee, S.H. and Ahn, Y., Upscaling of microfluidic fuel cell using planar single stacks, *Int. J. Energy Res.*, 2019, vol. 43, p. 5027.
14. Marschewski, J., Ruch, P., Ebejer, N., Kanan, O.H., Lhermitte, G., Cabrol, Q., Michel, B., and Poulidakos, D., On the mass transfer performance enhancement of membraneless redox flow cells with mixing promoters, *Int. J. Heat Mass Transfer*, 2017, vol. 106, p. 884.
15. Ferrigno, R., Stroock, A.D., Clark, T.D., Mayer, M., and Whitesides, G.M., Membraneless vanadium redox fuel cell using laminar flow, *J. Amer. Chem. Soc.*, 2002, vol. 124, p. 12930.
16. Feali, M.S. and Fathipour, M., An air-breathing microfluidic fuel cell with a finny anode, *Russ. J. Electrochem.*, 2014, vol. 50, p. 162.
17. Liu, Z., Ye, D., Chen, R., Zhang, B., Zhu, X., and Liao, Q., A dual-functional three-dimensional herringbone-like electrode for a membraneless microfluidic fuel cell, *J. Power Sources*, 2019, vol. 438, p. 227058.
18. Probststein, R.F., *Physicochemical Hydrodynamics: an Introduction*, 2nd ed., New York: John Wiley&Sons, 2003.
19. Chang, M.H., Chen, F., and Fang, N.S., Analysis of membraneless fuel cell using laminar flow in a Y-shaped microchannel, *J. Power Sources*, 2006, vol. 159, p. 810.